Particle Accelerators
1973, Vol. 5, pp. 207–214

A SHORT ELECTRON LINAC OF SIDE-COUPLED STRUCTURE WITH LOW INJECTION VOLTAGE

KATSUHIRO ONO, KOJI TAKATA† and NAOSHI SHIGEMURA

Toshiba Tamagawa Works, Tokyo Shibaura Electric Co., Ltd., 30 Hisamoto, Takatsu-Ku, Kawasaki, Japan

An electron linac with an overall length of 35 cm only has been constructed for medical use. The accelerating tube is a side-coupled structure with $Z_{eff}/Q = 6350\Omega/m$, where 2 bunching cells trap electrons well with the injection voltage as low as 5 kV. With an input power of 2 MW from a 3-GHz magnetron, 4-MeV, 100-mA beam pulses with 2 μs duration are obtained, where the beam diameter is 1 mm without any focusing magnet. The structure and the gun with an oxide cathode are sealed off together and evacuated by a 1 liter/s ion pump.

1. INTRODUCTION

Recently electron linacs have been frequently used for the treatment of cancer, and it has become desirable to make the accelerating structure short enough for easy and efficient handling in radiation therapy. For such a short linac, the accelerating structure must have an optimum shunt impedance, the bunching section must be well designed to minimize the phase slip between electrons and the rf field, and the gun and target system must be small enough.

In this paper, the construction of a short linac with the above characteristics is described. The electron acceleration experiment by an alternating periodic structure (APS) was discussed in a previous paper.[1] The shunt impedance of the APS is not so high, and therefore, after trials of several types of test cavities, a side coupled structure with a comparatively high impedance was chosen.

The linac is 31 cm long and consists of 7 accelerating cavities, 5 of which form a regular section ($\beta = 1.0$) and 2 of which are a buncher section. With a 2998 MHz microwave power of 1.8 MW, it accelerates electrons up to 4.6 MeV.

Particular attention is paid to the design of the buncher section and the electron gun in order to make the total length as short as possible. The buncher can trap electrons with an energy as low as 5 keV. This low injection voltage makes the size of the gun small. Furthermore, the beam is focused well by the electrodes in the gun and no focusing coil is used.

† National Laboratory for High Energy Physics, Oho-Machi, Tsukuba-Gun, Ibaraki, Japan.

The test cavity measurements, the analysis of the buncher section, the design of the whole structure and gun are described in the following, and these are compared with the experimental results.

2. ACCELERATING CAVITY

2.1. *General Description*

The shunt impedance per unit length measures the efficiency of a structure. For a standing wave linac it is defined as

$$Z_{eff} = \left[\frac{1}{L}\int_{-L/2}^{L/2} E(z)\cos(\pi z/L)\,dz\right]^2 \Big/ P_0, \quad (1)$$

where L is the cell length, P_0 the rf power dissipated in the cell, $E(z)$ the axial electric field.

The quantity Z_{eff}/Q, which depends on the cavity geometry only, is obtained for several types of the structure at $2850 \sim 3000$ MHz, where $E(z)$ is measured by the perturbation technique[2,3] with a metal bead of 4 mm in diameter.

For the electrically coupled alternating periodic structure (APS) of the previous paper, $Z_{eff}/Q = 2500\Omega/m$ and $Q = 9500$. The quantity Z_{eff}/Q is improved up to $2700\Omega/m$ by adding nose cones around the coupling hole on the disk. But there are limits to the improvement of Z_{eff} by this method, because a larger hole, which is required to increase the rf coupling suppressed by the nose cone, rather reduces the electric field along the central axis.

This defect is solved by coupling the cavities with the magnetic field through slots at the side wall of the cavities. For instance, Z_{eff}/Q of a magnetically coupled APS has been observed to be as high as

4500Ω/m at 2998 MHz, where the ratio of the length of the accelerating and coupling cell is 8.1 : 1.[4]

But further increase of the impedance is expected, if the coupling cell is shifted from the axis and, therefore, the accelerating cell becomes longer. Investigation of this side coupled structure[5,6] is reported in the present article.

2.2. *Side Coupled Structure*

As regards the structure shown in Figure 1, test cavity measurements have been carried out for the case $\beta = 1.0$. The radius of curvature R_1 of the side wall, the angle θ and radius of curvature r of the nose cone, the diameter of the beam hole d, and the cell length L are fixed at

$$R_1 = 23.5\,\text{mm}$$
$$\theta = 30°$$
$$r = 2.0\,\text{mm}$$
$$d = 6.0\,\text{mm}$$
$$L = 50\,\text{mm}$$

The coupling hole is 25 mm long and 11.5 mm wide on the side wall. The coupling cavity is a re-entrant type with a length of 30 mm and a diameter of 54 mm. The frequency is tuned by posts with a diameter of 8 mm on the axis.

For various values of the height H, the resonant frequency of the $\pi/2$ mode is kept constant at 2998 MHz by changing the radius R. The field of this mode is measured for the structure with two full accelerating cells and two electrically shorted half cells at both ends.

The variation of Z_{eff}/Q with H is shown in Figure 2. The maximum is 6350Ω/m at $H = 10$ mm. The

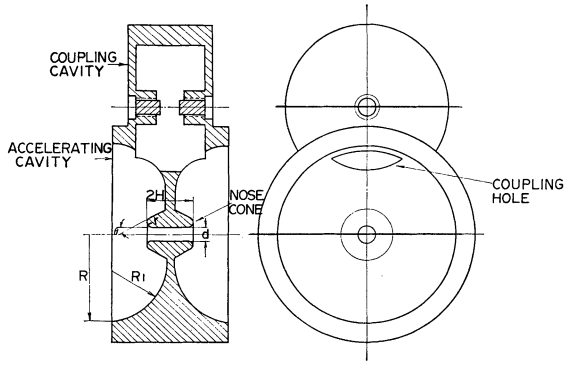

FIGURE 1 Cross section of a side-coupled accelerator structure.

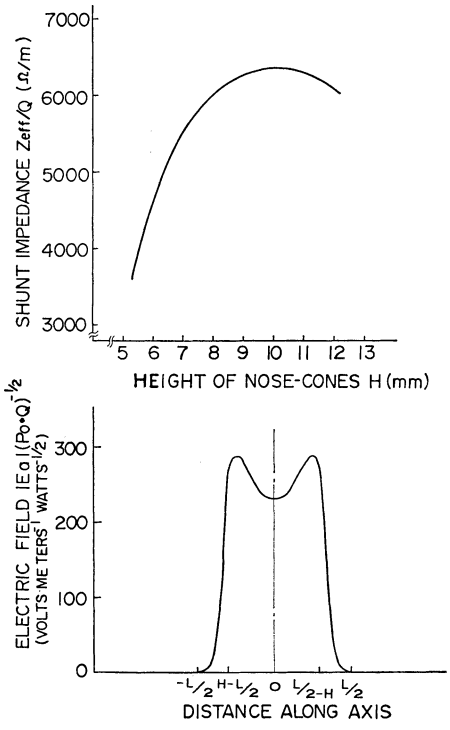

FIGURE 2 Variation of shunt impedance with the height of nose cones, and axial electric field measured in the optimized structure.

electric field for this H is shown also in Figure 2. This optimum geometry was adopted for the present accelerator.

3. BUNCHING CHARACTERISTICS

3.1. *General Description*

The injection with a low voltage makes the size of the gun very small. In the buncher design special attention is paid to trapping and acceleration of low energy electrons in a length as short as possible.

To determine the field distribution in this section, computer analyses were carried out with the following equations

$$eV = eV_{\text{inj}} + Re\left\{\int_0^z eE(z)\exp\left[i\left(\frac{\pi}{2} - \phi\right)\right]\mathrm{d}z\right\}$$
$$= m_0 c^2\left\{\left[1-\left(\frac{v}{c}\right)^2\right]^{-1} - 1\right\}$$
$$z = \int_0^t v\,\mathrm{d}t$$
$$\phi = \phi_{\text{inj}} + \omega t, \qquad (2)$$

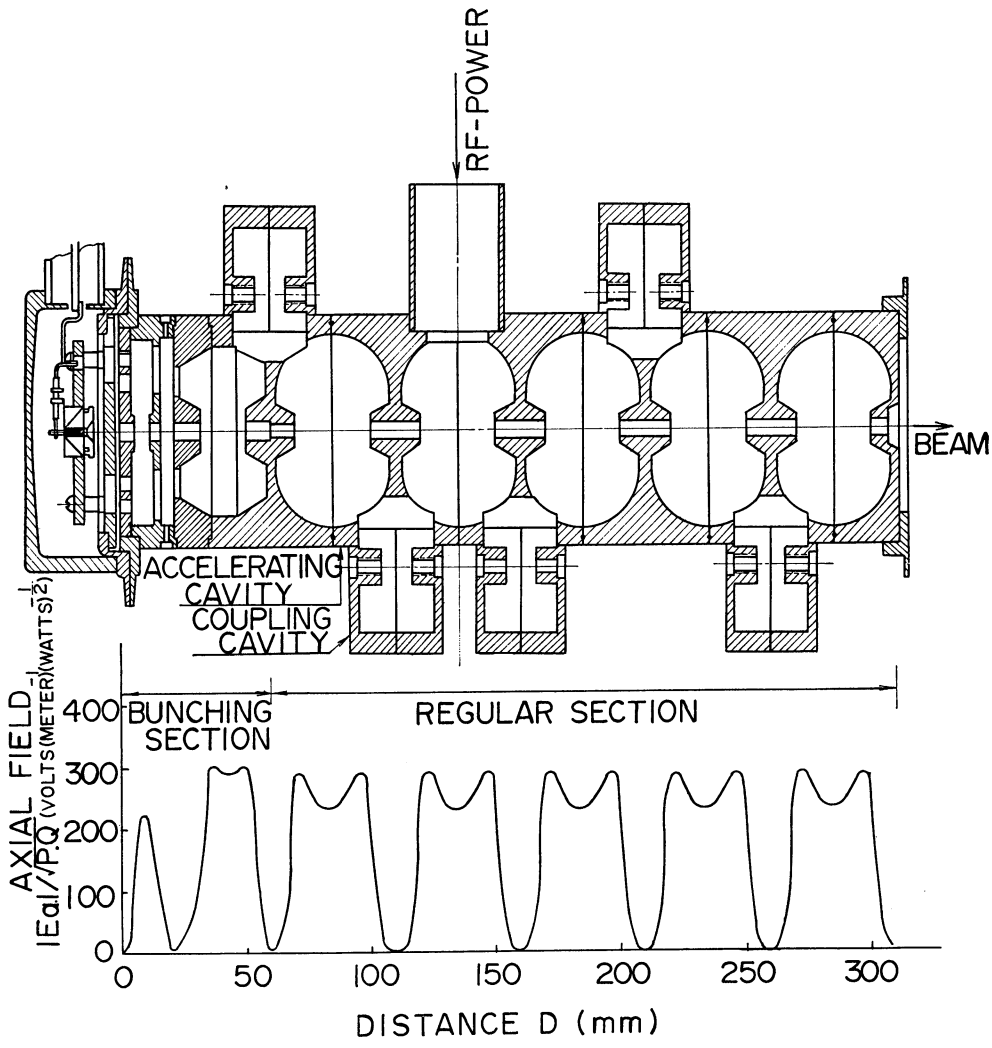

FIGURE 3 A cross-sectional view of the accelerator, including an electron gun, and a field distribution along the axis.

where eV is the kinetic energy of electrons, ϕ, z, v, their phase, position, and velocity respectively at time t, V_{inj} and ϕ_{inj} the injection voltage and phase, $E(z)$ the peak electric field, and c the velocity of light.

As to the field distribution in the buncher section, it is assumed, for simplicity, to be similar to that of the regular section shown in Figure 2, i.e.,

$$E(z) = E_n f\left(\frac{z-z_n}{\beta_n L_0}\right), \quad |z-z_n| \leqq \beta_n L_0/2,$$

where E_n is the amplitude, z_n the center, $\beta_n L_0$ the length of the *nth* cell, and L_0 ($= \lambda/2$) the length of the regular cell.

With the input power of 1.8 MW and Z_{eff} of 75 MΩ/m, and also with no phase slip between electron and the microwave field it requires $\sim$ 20 cm in order to obtain $\sim$ 5 MeV, which means 4 regular cells at least. By keeping every E_n same in the calculation, it is found that, for the desired operating condition $P_0 = 1.8$ MW, $V_{\text{inj}} = 22.5$ kV ($\beta = 0.29$), and $V = \sim 5$ MeV, the best bunching characteristics are obtained with 2 buncher cells having the following values of β:

$$\beta_1 = 0.4, \quad \beta_2 = 0.9,$$

and with 5 regular cells.

3.2. *Numerical Analysis of the Constructed Structure*

The structure which is constructed according to Section 3.1. is shown in Figure 3. The amplitude E_1 is not so high as others, because this cavity is coupled with the second accelerating cavity by a slotted cavity between them, and with this configuration the highest impedance cannot be attained as described in Section 2.1. This decrement is compensated by increasing E_2 higher than in other cells.

As regards the field of Figure 3, energy spectra are calculated for various values of P_0 and V_{inj}, where the beam loading is not considered.

In the case of $V_{inj} = 22.5$ kV, the spectrum, shown in Figure 4, is best at $P_0 = 1.5$—2.5 MW, but becomes worse at higher or lower P_0. The mean energy of the bunch divided by $P_0^{1/2}$ is fairly constant at 1—2 MW, but become lower at other power levels. These properties indicate the bunch is accelerated at the crest of the rf field throughout the structure for these power levels.

The effect of V_{inj} in the case of $P_0 = 1.8$ MW is shown in Figure 5. The mean energy and spectrum are almost unaffected for $V_{inj} = 5$—35 kV, but the trapping efficiency becomes small for low V_{inj}.

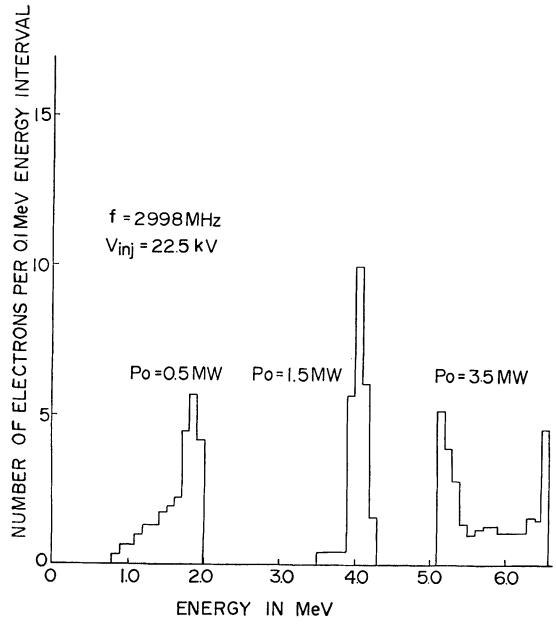

FIGURE 4 The energy spectrum of the electron beam. Electrons are injected into the accelerator in Figure 3 with an initial energy of 22.5 keV.

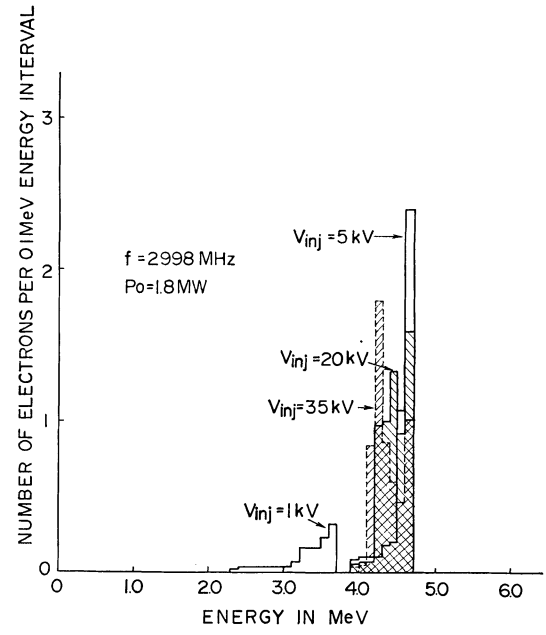

FIGURE 5 The energy spectrum of the electron beam. Initial energy is changed from 1 keV to 35 keV.

Thus the structure can accelerate electrons with good spectrum ($\sim 10\%$) and trapping efficiency ($\sim 30\%$) for the desired value of $P_0 = 1.8$ MW and $V_{inj} = 22.5$ kV. The first cavity needs no more side coupling though the impedance is not optimum, and therefore the manufacture of the structure becomes very easy.

4. ELECTRON GUN

The details of the gun are shown in Figure 3. Because about 30 per cent of the injection current is trapped as discussed in the previous section, the cathode emission must be about 500 mA to obtain accelerated currents of more than 100 mA.

A barium-impregnated oxide cathode with a diameter of 3.6 mm is used, which is mounted on a ceramic board with a thin molybdenum cylinder serving as a thermal shield for the heater. The anode with a beam aperture of 2.5 mm diam. is 9 mm distant from the cathode. Around the cathode is a focusing electrode with the same potential.

By tracing the beam orbits numerically for the case of $V_{inj} = 22.5$ kV, the best shape of the focusing electrode was sought. The beam can be

focussed up to 0.9 mm diam. at a point 24 mm distant from the cathode, which corresponds to the center of the first cell. As the electrons are accelerated very fast to relativistic energy and the space-charge effect is negligible for this range of current, the beam is expected to diverge very little at the output without any focusing magnet.

5. FABRICATION OF THE STRUCTURE

5.1. *Tuning Process*

Each accelerating cavity is tuned within 2998.0 ± 0.5 MHz, before attaching the coupling cavities. The resonance is monitored by a pair of antenna probes inserted into the beam hole. Then the coupling cavities are mounted on the structure, which are tuned also within the same frequency range by adjusting the gap of the posts. The frequency of the accelerating mode is not shifted by this attachment beyond the tuning accuracy.

After each cavity is tuned, the structure is brazed together (Figure 6), where errors of about 0.5 MHz are induced which, however, are not further corrected.[7]

The dispersion relation is plotted in Figure 7. The accelerating mode is spaced from the neighboring modes with nearly the same spacing, which secures the confluent condition. From this figure the contribution of the nonresonant modes at the initial stage of the build-up of the resonant mode is estimated at less than 5 per cent for the step-function driving pulse.[8] This is experimentally verified in Figure 8.

5.2. *Optimum Coupling*

The coupling between a waveguide and a standing wave linac affects the beam energy, which in the presence of beam loading, is given by[9,10]

$$V = [2(KP_0 Z_{\text{eff}} L_0)^{1/2} \cos\psi - Z_{\text{eff}} L_0 \cos^2\psi I_{\text{beam}}]/(1+K), \qquad (3)$$

where P_0 is the rf power, L_0 the length of an accelerator, I_{beam} the beam current, ψ the phase of electrons referred to the particular phase which would yield the maximum energy gain.

The coupling coefficient which maximizes the

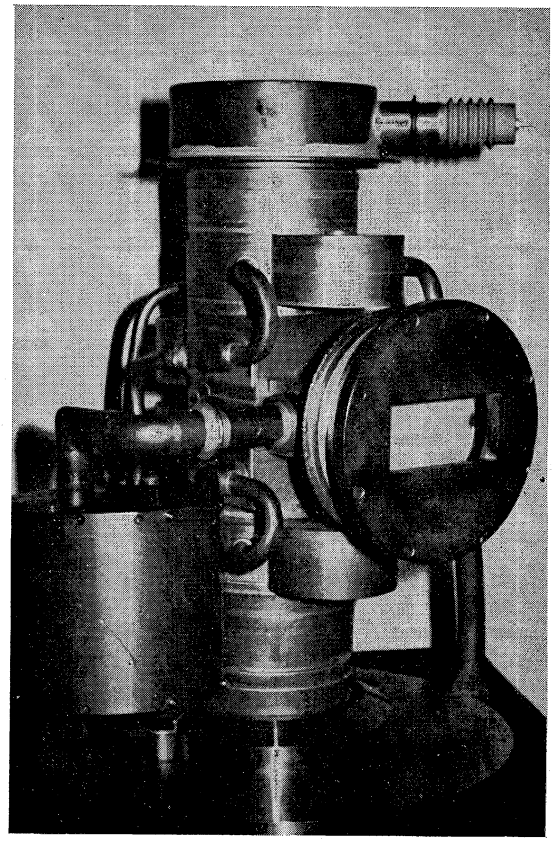

FIGURE 6 Photograph of the accelerator.

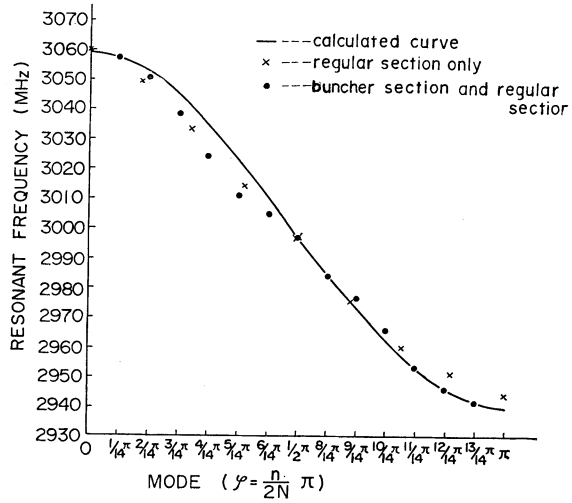

FIGURE 7 Dispersion relation for the accelerator.

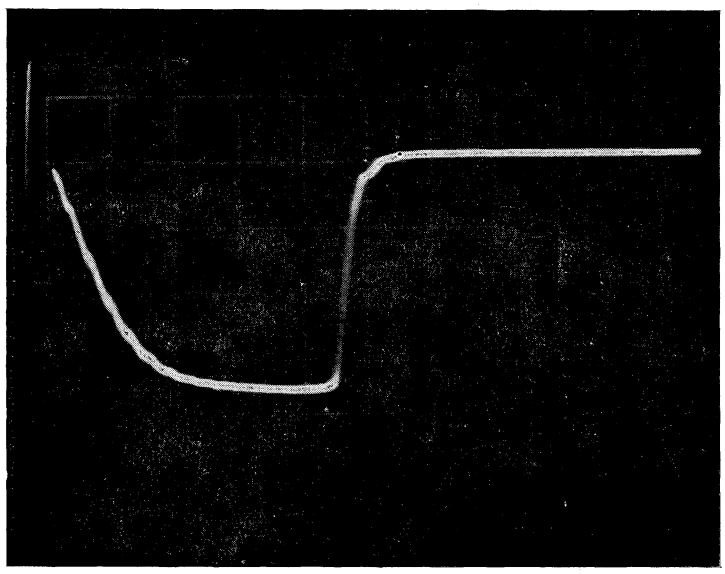

$\pi\frac{1}{2}$ mode

$f=2998$ MHz

0.5 μs/div

FIGURE 8 Amqlitude response at the center of a side-coupled cavity. Observed by a pick-up antenna in a cold test.

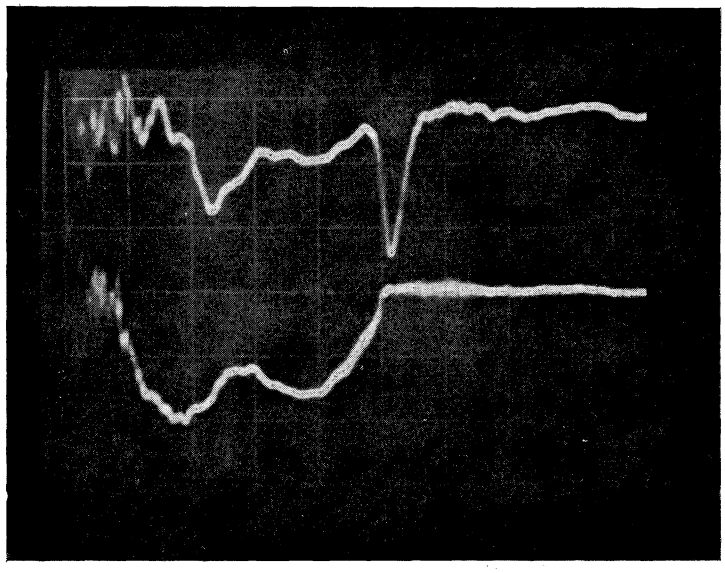

Reflected rf Power

Accelerated Electron Beam

$I_{beam}=100$ mA

$P_o=1.8$ MW

$V_{inj}=18$ kV

0.5 μs/div

FIGURE 9 The waveforms of beam current and reflected rf power.

energy V at a given current is described by the equation $dV/dK = 0$, that is,

$$K_{opt} = 1/4\{(Z_{eff} L_0/P_0)^{1/2}(I_{beam}\cos\psi) + [4+(Z_{eff} L_0 \cos^2\psi I_{beam}^2/P_0)]^{1/2}\}^2.$$

As this accelerator is used for I_{beam} of $\sim$ 100 mA and $\cos\psi$ of ~ 0.72, K is determined to be 1.3 by the above equation.

It may be desirable that K is a little larger than the above value in the case of pulse drive, as the field builds up like $E\{1-\exp[-(1+K)\omega t(2Q_0)^{-1}]\}$. This is not considered in this paper for simplicity.

6. EXPERIMENTS

6.1. *General Description*

The accelerator is driven by the tunable magnetron M190 of the Japan Radio Company or M5015 of the English Electric Valve Co. These can generate maximum peak power of 2 MW. A circulator TOSHIBA FCS-51 with an isolation of 23 dB and an insertion loss of 0.5 dB is inserted between the magnetron and the accelerator. The rf frequency is adjusted to the resonant frequency of the accelerator with an automatic frequency control system, which detects the change of phase of the reflected microwave and feeds it back to a mechanical tuner.

Two line pulse modulators are used, one of which generates 45 kV for the magnetron and the other for the electron gun. The pulses from the two modulators have the same width (2.5μs) and timing.

6.2. *Output Beam* (see Figure 9)

The beam size is monitored at the output window with a plastic dosimeter whose colour changes with irradiation of electrons. This indicates that the diameter of the beam is within 1 mm although no focusing magnet is used.

The energy of the electrons is estimated by measuring the maximum mean-path in acryl or water according to the following equation[11]

$$R \cdot S(z/a)_{eff} = 0.285\, V - 0.137, \qquad (4)$$

where R is the maximum mean-path of the electrons in centimeters, V the energy of the electrons in MeV, and $S(z/a)_{eff}$ is a parameter which depends on the material. For instance, $S(z/a)_{eff} = 0.577$ for water and $S(z/a)_{eff} = 0.635$ for acryl. The results are plotted in Figure 10 and compared with the beam loading curve which is given by Eq. (3)

$$V(\text{MeV}) = 3.43(P_0(\text{MW}))^{1/2} - 5.3 I_{beam}(\text{A}) \qquad (5)$$

for $Z_{eff} = 75$ MΩ/m, $L_0 = 0.31$ m, $K = 1.3$ and $\cos\psi = 0.72$.

Figure 10 shows that the beam energy without loading is equal to 4.6 MeV and that with loading of 0.1 A to 4.1 MeV, which agrees well with Eq. (5).

This was also confirmed with an X-ray experiment by measuring the depth in water where the dose rate of X-rays falls to 1/2. In this experiment, the half dose rate depth is 13.0 cm in water for $P_0 =$ 1.8 MW and $I_{beam} = 0.113$ A. This shows that the

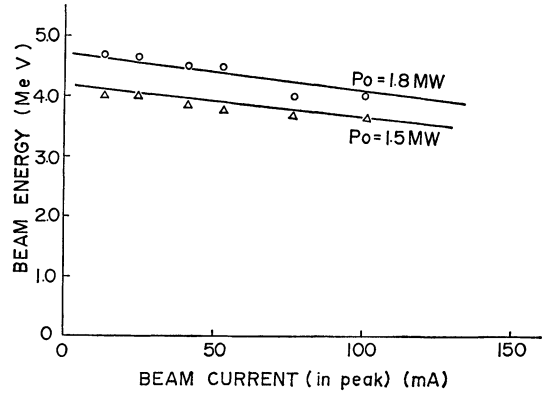

FIGURE 10 Beam loading characteristics.

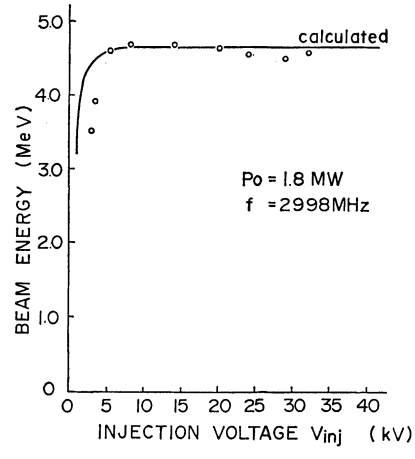

FIGURE 11 Variation of beam energy with respect to the initial energy of electrons.

beam energy in this condition is equal to 4.0 MeV according to the standard data.[12]

The beam energy for an injection voltage between 3 and 35 kV, where $P_0 = 1.8$ MW, is shown in Figure 11, and compared with the calculated curve. This shows that the energy is not affected by the injection voltage in the range from 5 kV to 35 kV.

The ratio of accelerated electrons to injected electrons is shown in Figure 12 and compared with the calculated curve. The observed electrons are fewer than the calculated ones by about 10 per cent which may be due to loss at the titanium output window and to the calculation based on the cw drive.

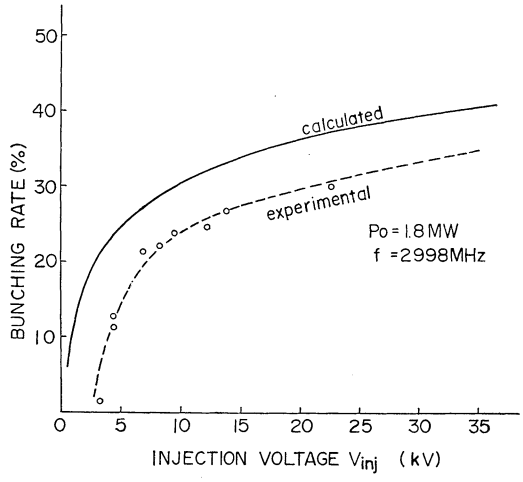

FIGURE 12 The ratio of accelerated electrons to the injected electrons.

REFERENCES

1. T. Kikuchi and K. Takata, *Japan. J. Appl. Phys.* **9,** 679 (1970).
2. L. C. Maier, Jr. and J. C. Slater, *J. Appl. Phys.* **23,** 68 (1952).
3. L. C. Maier, Jr. and J. C. Slater, *J. Appl. Phys.* **23,** 78 (1952).
4. K. Ono, T. Kikuchi and K. Takata, Rep. on the Meeting of the Soc. of Appl. Physics of Japan, No. 1 (1970), p. 41 (in Japanese).
5. E. A. Knapp, B. C. Knapp and J. M. Potter, *Rev. Sci. Instrum.* **39,** 979 (1968).
6. K. Irie, Y. Minowa and S. Sowada, *Japan. J. Appl. Phys.* **12,** 277 (1973).
7. B. C. Knapp, E. A. Knapp, G. J. Lucas and J. M. Potter, *IEEE Trans. Nucl. Sci.* **NS-12,** No. 3, 159 (1965).
8. T. Nishikawa, *Linear Accelerators*, ed. P. M. Lapostolle and A. L. Septier (John Wiley & Sons, New York, 1970), pp. 809–826.
9. G. A. Loew and R. B. Neal, *Linear Accelerators*, ed. P. M. Lapostolle and A. L. Septier (John Wiley & Sons, New York, 1970), pp. 39–113.
10. G. Dôme, *Linear Accelerators*, ed. P. M. Lapostolle and A. L. Septier (John Wiley & Sons, New York, 1970), pp. 637–738.
11. B. Markus, *Strahlen Therapie* **116,** 280 (1961).
12. D. E. A. Jones *et al.*, *Brit. J. of Radiol.*, Suppl. 10, p. 59.

Received 22 June 1973